Supplementary Information (SI) for Physical Chemistry Chemical Physics.
This journal is © the Owner Societies 2026

Supplementary information for

Strategy for Steganography and Information Encryption-decryption using fs laser-created Anisotropic-writable Luminescence in Organic Solids

Ruyue QUE[1], Olivier PLANTEVIN[2], Matthieu LANCRY[1], Bertrand POUMELLEC[1, *]

[1] Université Paris-Saclay, CNRS, Institut de chimie moléculaire et des matériaux d'Orsay, SP2M, 91405, Orsay, France.
[2] Université Paris-Saclay, CNRS, Laboratoire de Physique des Solides, 91405, Orsay, France.

*Corresponding author: bertrand.poumellec@universite-paris-saclay.fr

S1. Raw luminescence signal and its components, including system anisotropy and bleaching effect

Fig.S1a and Fig.S1b show the raw data of the intensity of photoluminescence in the same area of a Zeonex sample placed horizontally (0º) and vertically (90º), respectively. These 2 areas were created by fs laser irradiation without post-exposure process. Bleaching effect and system anisotropy is demonstrated in both positions. Particularly, the anisotropy in both figures with minimum intensity in 0º and maximum intensity in 90º implies that the system anisotropy dominant in the sample unexposed.

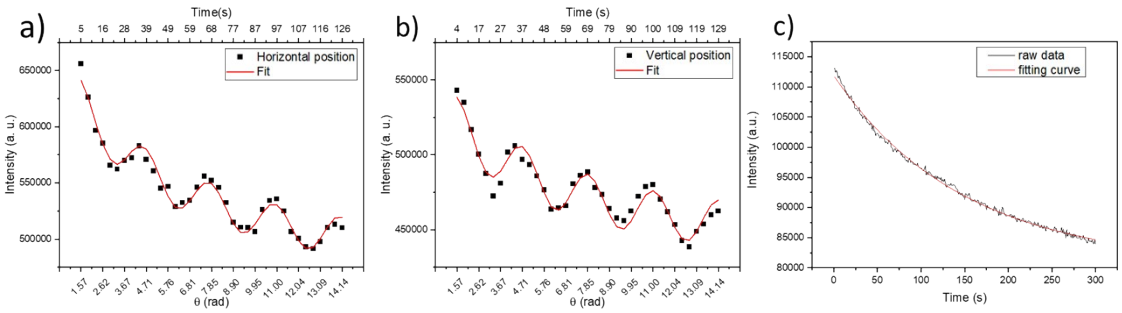

Fig. S1 (a)- (b)Photoluminescence intensity over time and probing polarizations of an area in fs laser-irradiated Zeonex sample posed (a) horizontally and (b) vertically. (c) Bleaching decay of fs-irradiated glycine sample under excitation of 448nm CW laser with intensity of 1.78mW/cm²

Therefore, we assumed that the photoluminescence comprises combination of (un)bleachable and (an)isotropic components, as described by Equation S1. The correspondent components are shown in Table S1. θ corresponds to the probing excitation polarization direction to system x-axis. θ_0 refers to the position of the minimum intensity. τ is the bleaching time constant. A_1 is a total amplitude coefficient. A_2 represents the coefficient of bleachable component, which is only related to material. A_3 is the coefficient of the anisotropic component. The fitting results in two measurement configurations (0º and 90º) above are shown in Table S2. Table S3 shows the proportion of the contribution of different components accordingly.

$$I(\theta,t) = A_1\left(1 + A_2.e^{-\left(\frac{t}{\tau}\right)}\right)\left(1 + A_3.sin^2(\theta - \theta_0)\right) \#Eq.S1$$

Table S1

Components	Expressions
non-bleachable-isotropic	A_1
bleachable-isotropic	$A_1.A_2.e^{-\left(\frac{t}{\tau}\right)}$
non-bleachable-anisotropic	$A_1.A_3.sin^2(\theta-\theta_0)$
bleachable anisotropic	$A_1.A_2.A_3.e^{-\left(\frac{t}{\tau}\right)}.sin^2(\theta-\theta_0)$

Table S2

Values	Horizontal position	Vertical position
τ (s)	58.3	62.0
A_1	470×10^3	430×10^3
A_2	0.304	0.184
A_3	0.0687	0.0679
θ_0(rad)	-0.091	0.0166

Table S3

Properties	Contributions
Total	100.0%
unbleachable isotropic	71.8%
Bleachable isotropic	21.8%
unbleachable anisotropic	4.9%
Bleachable anisotropic	1.4%

Results show a small difference of A_3 and θ_0 between the two configurations, indicating that the anisotropy arises mainly from the system (dichroic mirror), the material anisotropy induced by the fs laser irradiation is negligible. The variation of A_2 arises from a time shift of ~30s on the time origin and depend on the previous illumination between the two experiments.

In conclusion, in this experiment, we found that the system anisotropy is 4.9%. Using expression Eq. S1 and coefficient values Table S2, we can easily correct for bleaching effects and system anisotropy in the raw data.

In addition, the photobleaching effect was observed not only in the fs-laser irradiated Zeonex matrix but also in the fs-irradiated glycine samples. Fig.S1c illustrates the decay of the emission intensity at 510nm under 448nm CW laser excitation. The decay curve was fitted by $I(t) = A_1[1 + A_2 e^{-\left(\frac{t}{\tau}\right)}]$, with the fitting parameters: $A_1 = 80606.7(a.u.),\ A_2 = 0.39(a.u.), \tau = 147.4s$ (with standard error of 2.2s). It should be noted that the value of A_2 depends on the sample's exposure history (i.e. the chosen time origin). These results confirm the presence of two distinct components: a bleachable species and a stable, non-bleachable. The bleaching time constant appears to be material dependent (e.g. around 60s in fs-irradiated Zeonex).

Fitting parameters of Fig.3.The experimental data represented by the blue and red dots in Fig.3 were also fitted by Eq.S1. After correcting for the bleaching effects and system anisotropy, the extracted fitting parameters are listed in Table S4, while the corresponding contributions of isotropic and anisotropic components are detailed in Table S5. Notably, the value of A_3 significantly increased from 0.068 (unexposed data, see Table S2) to 0.245 following the writing (pre-exposure) process.

Table S4

Values	Area 1 (red)	Area 2 (blue)
τ (s)	∞	∞
$A1(1+A2)$	183×10^3	206×10^3
$A3$	0.245	0.134
θ_0(rad)	0.013	1.53

Table S5

Properties	Contributions	
	Area 1 (red)	Area 2 (blue)
isotropic	80.3%	88.2%
anisotropic	19.7%	11.8%

Independence of the luminescence spectral shape during bleaching and under different excitation polarization direction. We investigated the emission spectra of PL in fs laser irradiated glycine sample under 448nm excitation with different polarization direction, as shown in Fig.S2. The overall intensity decreases due to bleaching. In Fig.S2b, the spectra exclude bleaching effect and alter x-axis from wavelength to corresponding energy.

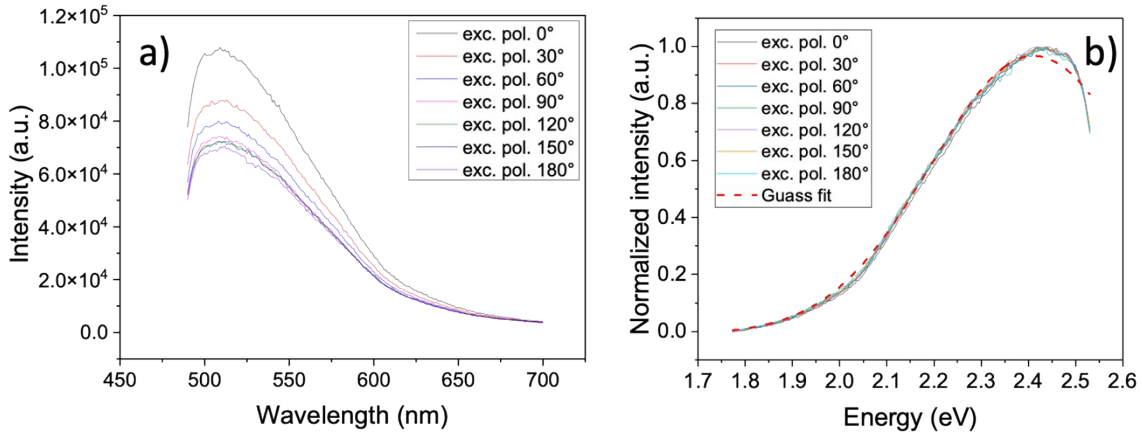

Fig.S2 The emission spectra of PL in α-glycine crystal under 448nm excitation with polarization varying from 0° to 180° with 30° step. Each spectral measurement took a period of 30s. a) The raw spectra data; b) The corresponding normalized spectra with x-axis altered on photon energy; The red dash line is a single Gaussian curve fit.

From Fig.S2b. nearly no distortion of the spectra is observed while bleaching and altering excitation polarizations. It can be fitted with a single Gaussian curve with the maximum at 2. 41eV, bandwidth of 0.22eV (at $1/e^2$) which is quite common for organic luminescence centers [1]. Therefore, only one luminescent specie was involved during the bleaching process, as well as in the measurements according to different excitation polarizations. Similar results were shown in another organic compound [2].

S2. More results in other materials and other excitation polarization angles

Fig.S3 displayed that using fs laser irradiation with proper parameters, PL can be locally induced not only in Zeonex polymer, but also glycine single crystal and sucrose single crystal. As shown in Fig.S3e, the emission spectra of the PL in these 3 materials under 448nm excitation have a maximum around 510nm, while the unirradiated samples appear no luminescent at this excitation wavelength. Therefore, this wavelength is applied for detection in this experiment.

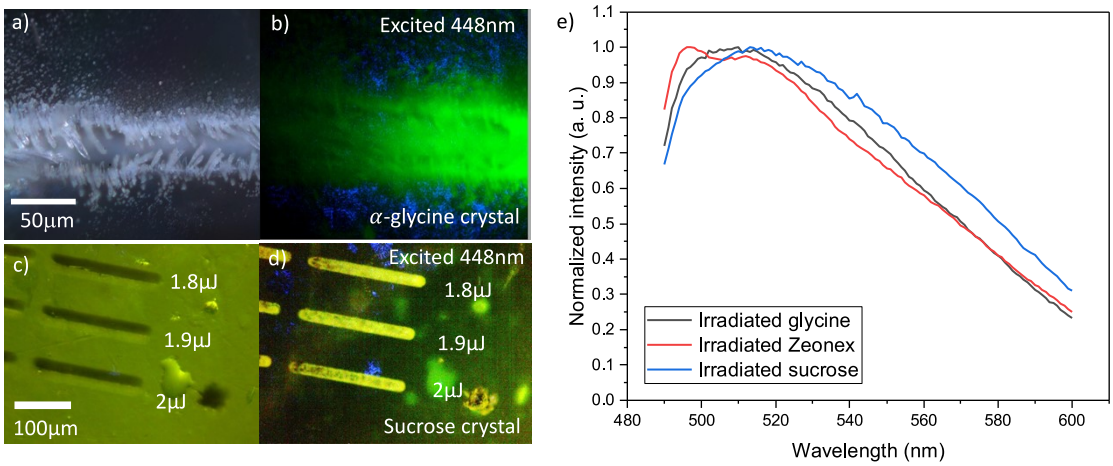

Fig.S3: a)-b) Fs-laser irradiated trace on α-glycine crystal. Fs laser parameters: 1.7 μJ, 1MHz, 2μm/s. a) Microscope image on reflection mode with polarized light illumination, analyzer is applied and oriented to be perpendicular to the illuminating polarization. b) Luminescent image of corresponding trace, excitation on 448nm. c)-d) Fs-laser irradiated traces on sucrose crystal. Fs laser parameters: 1.8-2μJ, 1kHz, 10μm/s. c) Microscope image in transmission mode, illumination with natural light. d) Luminescent image of corresponding traces, excitation on 448nm. e) The emission spectra of fs laser-generated PL in glycine, Zeonex and sucrose sample excited by 448nm laser.

The property of controllable excitation anisotropy was observed also in this fs laser-induced photoluminescence in α-glycine single crystal and sucrose single crystal samples.

Different polarization angles were applied in the post-exposure process with other as-cast areas, as shown in Fig.S4. Results show that after post-exposure process, the PL intensity varies according to the excitation polarization direction, i.e. excitation anisotropy. In addition, this anisotropic property is dependent on the post-exposure polarization, where **the minimum appears always at the angle of post-exposure polarization and the maximum is at the angles perpendicular to the post-exposure polarization**. As the anisotropic properties can be encoded respecting to the polarization direction of the laser light in the post-exposure, this process is called the 'writing step'. To quantity the extent of this anisotropic property, excitation polarization degree (EPD) is defined as $EPD = \frac{I_{max} - I_{min}}{I_{max} + I_{min}}$ [3]. The comparison of the results in 3 materials show that the writing efficiency is of the same order although the molecular structure, the long-range order, and the chemical compositions of these 3 materials are quite different.

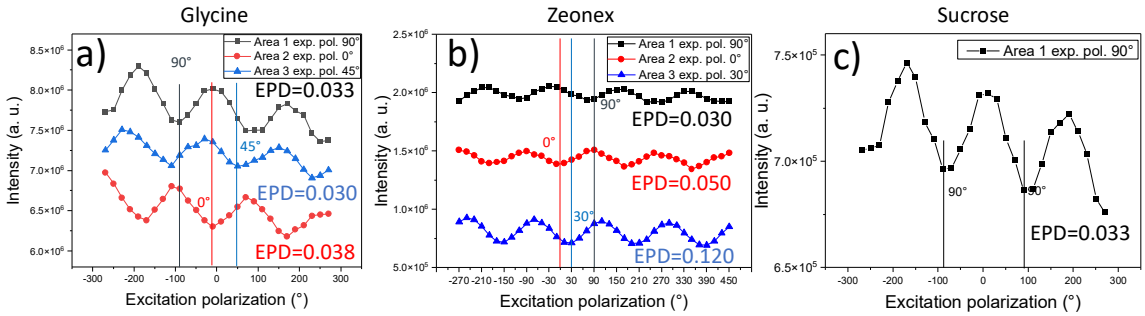

Fig.S4: PL intensity with respect to excitation polarizations in (a) glycine crystal, (b) Zeonex glass and (c) sucrose crystal. PL The PL in the 3 cases is excited at 448nm and detected at 510nm from different areas after 2 min post-exposure. For (a), the fs laser irradiation conditions: 1MHz, 1.7μJ, 1μm/s. The post-exposures are under polarization of 0°, 45° and 90°. For (b), the fs laser irradiation conditions: 500kHz, 50nJ, speed=10μm/s. Post-exposure under polarizations of 0°, 30° and 90°.For (c), the fs laser conditions: RR=1kHz, Ep=2μJ, scanning speed=10μm/s.

This anisotropic property in one area can be altered by re-exposure to another polarization, so-called 'rewriting step', is also observed in glycine and sucrose crystal. After imprinting anisotropy in an area in a given direction, if one performs a second exposure with another direction of polarization, the emission intensity minimum is then shifted to be at the new polarization direction, or simply became less anisotropic depending on the materials and exposure time, as shown in Fig.S5.

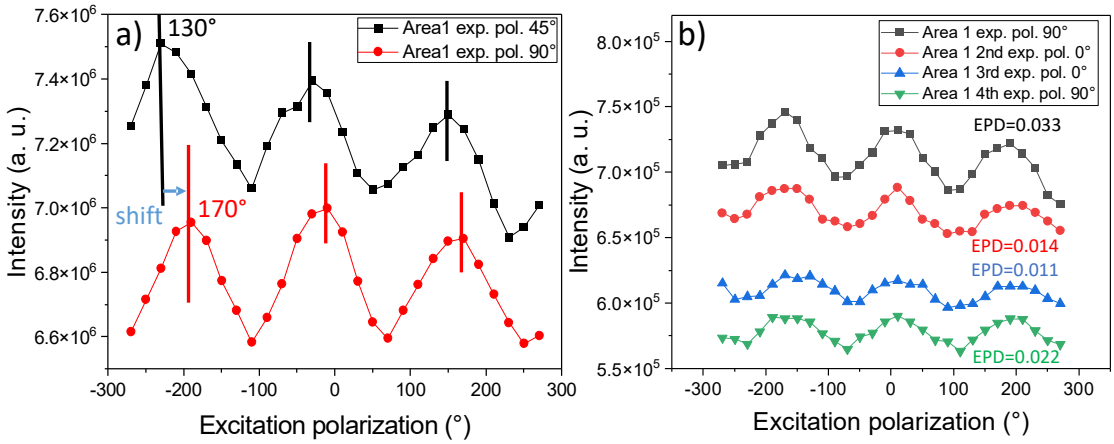

Fig. S5: Rewriting results in (a) glycine and (b) sucrose crystal. Post-exposure process was performed under linear polarized laser of 448nm in one area. For (a), the exposure was under polarization of 45° and then 90°. For(b), the post-exposure process was performed with 4 steps alternating between 90° and 0°.

S3. ANISOTROPY THEORY

The microscopic origin of the observable excitation anisotropy

In the absence of photobleaching, the luminescence intensity is described through a quasi-chemical reaction scheme involving molecular excitation and relaxation:

$$A \underset{+h\nu_e,\ k_e}{\overset{-h\nu_a,\ k_a}{\rightleftarrows}} A^* \#(Eq.S2)$$

Here, A and A^* denote the molecules in the ground and excited states, respectively. The absorption (k_a) and emission (k_e) transition rates depend on the molecular electronic structure and photon energies ($h\nu_a$, $h\nu_e$).

The absorption rate k_a is governed by the interaction between the molecule transition dipole d and the excitation field E_a, described by the dipole term in the hamiltonian: $\hat{D}_a = E_a \cdot \hat{d} = E_a e_a . \hat{d}$, where E_a is the amplitude and e_a is the polarization unit vector of the incoming field.

Thus, the absorption rate is then given by:

$$k_a(h\nu_a) \propto \left|\langle \psi_{exc} \left| \hat{D}_a \right| \psi_g \rangle\right|^2 \delta\left(E_{\psi_{exc}} - E_{\psi_g} - h\nu_a\right) \#(Eq.S3)$$

Where ψ_g is the vibronic wavefunction of the electronic ground state and $\psi_{exc}$the vibronic wavefunction of the excited state. As vibrations are quite small with the light field intensity we used, the matrix term $\langle \psi_{exc} \left| \hat{D}_a \right| \psi_g \rangle$ is just dependent on the laser polarization through the molecular electronic structure that is constant within the absorption band into consideration. Furthermore, due to narrow bandwidth of exciting wavelength that we use, the transition selectively populates a single vibrational level of the excited state A^* [4].

By expressing the field amplitude in terms of the probing light intensity $I_{prob} = n\varepsilon_0 c E_a^2/2$, we obtain k_a:

$$k_a(h\nu_a) \propto I_{prob} \cdot \left|\langle \psi_{exc} \left| e_a \cdot \hat{d} \right| \psi_g \rangle\right|^2 \delta\left(E_{\psi_{exc}} - E_{\psi_g} - h\nu_a\right) \#(Eq.S4)$$

Crucially, the dependence on excitation polarization e_a arises from the transition matrix element $\langle \psi_{exi} \left| e_a . \hat{d} \right| \psi_g \rangle$, whose value depends on the alignment between the polarization direction and the molecular transition dipole, and is nonzero only when symmetry allows [5-7].

After excitation, electrons at the excited vibrational levels corresponding to $h\nu_a$ relax to the lowest vibration excited electronic states, denoted as ψ_{emig}. From this level, excited molecules relax to any vibrational levels (indexed v) of the lowest electronic configuration (the same of the ground states). This is the emission process at the light energy $h\nu_e$, leading to:

$$I_{lum}(h\nu_e) \propto k_e(h\nu_e)[A^*] \#(Eq.S5)$$

We obtain thus the emission transition rate k_e:

$$k_e(h\nu_e) \propto I_{lum} \cdot \left|\langle \psi_v \left| e_e \cdot \hat{d} \right| \psi_{emig} \rangle\right|^2 \delta\left(E_{emig} - E_{\psi_v} - h\nu_e\right) \#\#(Eq.S6)$$

Due to the multiplicity of the vibration levels, the relaxed A* molecules are distributed. As we do not select the luminescence wavelength, we have to sum on the relevant band and thus the total emission transition rate is $\sum_{h\nu_e} k_e(h\nu_e)$.

The emission process for a given $h\nu_e$ is polarized if the emitting molecule is anisotropic, but in our experimental setup we have not analyzed this property.

Luminescence intensity and polarizations dependence

From above discussion, the luminescence intensity we collect is $I_{lum} \propto \sum_{h\nu_e} k_e(h\nu_e)[A^*]$ and the luminescence intensity is only dependent on $[A^*]$ that is dependent on $k_a(h\nu_a)$ containing the incoming polarization dependence. We have thus to compute the excited-state population $[A^*]$. The system kinetics are described by:

$$\frac{d[A^*]}{dt} = k_a[A] - k_{-1}[A^*],\ [A] + [A^*] = A_0 \#(Eq.S7)$$

where k_{-1} represents the total relaxation rate (including both radiative and non-radiative channels).

Assuming $[A^*](t=0) = 0$, the solution is:

$$[A^*] = \frac{k_a.A_0}{k_a + k_{-1}}\left[1 - exp\left(-(k_a + k_{-1})t\right)\right] \underset{t \gg \frac{1}{k_a} + k_{-1}}{\rightarrow} \frac{k_a.A_0}{k_a + k_{-1}} \#(Eq.S8)$$

Assuming rapid relaxation, $k_{-1} \gg k_a$, the population simplifies to:

$$[A^*] \approx \frac{k_a A_0}{k_{-1}} \#(Eq.S9)$$

Substituting this into the intensity equation yields:

$$I_{lum}(h\nu_a, h\nu_e) \propto \frac{k_a(h\nu_a)k_e(h\nu_e)}{k_{-1}} A_0 \propto k_a(h\nu_a)PQY(h\nu_e)A_0 \#(Eq.S10)$$

Here, to isolate the polarization-dependent terms, we group the emission and relaxation factors into a single parameter, the Partial Quantum Yield,

$$PQY(h\nu_e) = \frac{k_e(h\nu_e)}{k_{-1}} \#(Eq.S11)$$

we obtain:

$$I_{lum}(h\nu_a, h\nu_e) \propto k_a(h\nu_a)PQY(h\nu_e)A_0 \#(Eq.S12)$$

(Note: The total quantum yield Q is simply the integration of PQY over the relevant emission band, i.e., $Q = \frac{\sum_{h\nu_e} k_e(h\nu_e)}{k_{-1}} = \sum_{h\nu_e} PQY(h\nu_e)$).

Consider a luminophore with reference axes X, Y, Z, an anisotropic response arises only if one axis (say, along angle φ) has a non-zero dipole transition moment. In the lab frame (x, y, z), with excitation polarization angle θ, the dipole coupling gives:

$$\langle \psi_{exc}(\varphi) \left| e_a \cdot \hat{d} \right| \psi_g \rangle = d(h\nu_a)\cos(\theta - \varphi) \#(Eq.S13)$$

and the absorption rate becomes:

$$k_a(I_{prob}, h\nu_a, \theta, \varphi) = I_{prob} \cdot \left[d_a(h\nu_a)\right]^2 cos^2(\theta - \varphi) \#(Eq.S14)$$

Assuming a luminophore orientation distribution $\frac{\delta A_0}{\delta \varphi}(\varphi)$, the luminescence intensity is:

$$\frac{dI_{lum}}{d\varphi}(I_{prob}, h\nu_a, h\nu_e, \theta, \varphi) \propto I_{prob} PQY(h\nu_e)\left[d_a(h\nu_a)\right]^2 cos^2(\theta - \varphi)\frac{\delta A_0}{\delta \varphi}(\varphi) \#(Eq.S15)$$

For one direction of laser polarization θ, the total luminescence intensity is obtained by integration over all directions of luminophore:

$$I_{lum}(I_{prob},h\nu_a,h\nu_e,\theta,\varphi) \propto I_{prob}PQY(h\nu_e)\int_0^{2\pi}[d_a(h\nu_a)]^2cos^2(\theta-\varphi)\frac{\delta A_0}{\delta\varphi}(\varphi)d\varphi \#(Eq.S16)$$

The term $[d_a(h\nu_a)]^2cos^2(\theta-\varphi) = R(h\nu_a,\theta,\varphi)$ is the response to the light probe of the luminophore direction distribution.

Thus, the total luminescence intensity can be expressed as:

$$I_{lum}(I_{prob},h\nu_a,h\nu_e,\theta) \propto I_{prob}PQY(h\nu_e)\int_0^{2\pi}R(h\nu_a,\theta,\varphi)\frac{\delta A_0}{\delta\varphi}(\varphi)d\varphi \#(Eq.S17)$$

If the luminophore orientation distribution is isotropic, i.e., $\frac{\delta A_0}{\delta\varphi}(\varphi) = constant$, the integral becomes independent on θ, and no excitation anisotropy is observed----as is the case in isotropic media such as liquids or glasses.

In conclusion, anisotropy arises only when both the luminophores are asymmetric and their orientation distribution is anisotropic, as described by Weigert's law [8]. If the luminophore's point group symmetry allows multiple non-zero dipole directions, the angular dependence is more complex, but the overall conclusion remains unchanged.

S4. THE BLEACHING EFFECT ON THE DISTRIBUTION

We assume that the observed anisotropy creation and reorientation arise from a bleaching process, in which the excited species A^* is partially transformed into another (likely thermally accessible) species B (*Eq.S18)*.

$$A \underset{+h\nu_e,\ k_e}{\overset{-h\nu_a,\ k_a}{\rightleftarrows}} A^* \xrightarrow{k_b,\ thermal} B \#(Eq.S18)$$

As the luminescence intensity is proportional to $[A^*]$ (*Eq.S6*), the bleaching pathway altered the population of $[A^*]$ over time. We therefore solve the following equations to describe its time evolution.

(1) $\frac{d[A^*]}{dt} = k_a[A] - k_{-1}[A^*] - k_b[A^*]$
(2) $[A] + [A^*] + [B] = A_0$
(3) $\frac{d[B]}{dt} = k_b[A^*]$

The boundary conditions are:

(1) $[A^*](t=0) = 0$
(2) $[B](t=0) = 0$
(3) $[B](t=\infty) = A_0$

Solving these equations gives:

$$[A^*] = \frac{2k_aA_0}{\sqrt{(k_a+k_{-1}+k_b)^2-4k_ak_b}}exp\left(\frac{-(k_a+k_{-1}+k_b)}{2}t\right)sinh\left(\frac{\sqrt{(k_a+k_{-1}+k_b)^2-4k_ak_b}}{2}t\right)$$

where $(k_a+k_{-1}+k_b)^2-4k_ak_b > 0$. Fig. S6 shows the time evolution of $[A^*]$, $[B]$ and $[A]$.

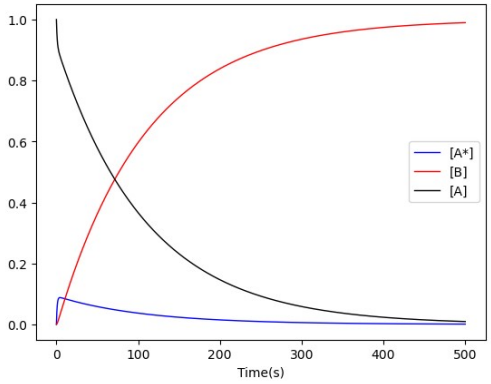

Fig. S6: $[A^*](t)$, $[B](t)$ *and* $[A](t)$ *with* $A_0 = 1, k_a = 0.1,\ k_{-1} = 0.9,\ k_b = 0.1$.

At short times, $[A^*](t)$ rises and then decays exponentially once the bleaching rate k_b dominates. Under the approximation $k_{-1} \gg k_a$, we can further simplify:

$$[A^*] = \frac{k_a A_0}{k_{-1} + k_b} exp\left(-\frac{k_a k_b}{k_{-1} + k_b} t\right)$$

Hence, the luminescence intensity is:

$$I_{lum}(h\nu_a, h\nu_e) \cong k_e(h\nu_e)[A^*] \approx k_a(h\nu_a, I_{prob}, \theta, \varphi)\frac{k_e(h\nu_e)}{k_{-1} + k_b} A_0 exp\left(-\frac{k_a k_b}{k_{-1} + k_b} t\right)$$

This exponential decay explicitly depends on the excitation polarization through $k_a(h\nu_a, I_{prob}, \theta, \varphi)$ as in Supplementary S3. Replacing $[A^*]$ by $\frac{\delta[A^*]}{\delta\varphi}(\varphi)$ and A_0 by $\frac{\delta A_0}{\delta\varphi}(\varphi)$ yields:

$$\frac{dI_{lum}}{d\theta}(\theta, \varphi) = k_a(h\nu_a, I_{prob}, \theta, \varphi)\frac{k_e(h\nu_e).}{k_{-1} + k_b} \cdot exp\left[-\frac{k_a k_b}{k_{-1} + k_b} \cdot t\right] \cdot \frac{\delta A_0}{\delta\varphi}(\varphi)$$

Recast in terms of the dipole response $R(h\nu_a, \theta, \varphi) = [d_a(h\nu_a)]^2 cos^2(\theta - \varphi)$ and partial quantum yield $PQY(h\nu_e) = \frac{k_e(h\nu_e)}{k_{-1} + k_b}$

$$I_{lum}(h\nu_a, h\nu_e, \theta) = I_{prob} PQY(h\nu_e) \int_0^{2\pi} R(h\nu_a, \theta, \varphi) exp\left(-\frac{I_{prob}.R(h\nu_a, \theta, \varphi) k_b}{k_{-1} + k_b} t\right) \frac{\delta A_0}{\delta\varphi}(\varphi) d\varphi$$

.

The bleaching function is $f(t, I_{prob}, R(h\nu_a, \theta, \varphi)) = exp\left(-\frac{I_{prob}.R(h\nu_a, \theta, \varphi) k_b}{k_{-1} + k_b} t\right)$. Because k_b is not dependent on θ (thermal reaction), if $\frac{\delta A_0}{\delta\varphi}(\varphi)$ is isotropic, no net anisotropy appears.

Writing process: directional post-exposure process

If the sample is exposed to a linearly polarized laser at polarization θ_1 for a duration t_1, the absorption rate for luminophores at orientation φ is $k_a(h\nu_a, I_{expo}, \theta_1, \varphi) = I_{expo}[d_a(h\nu_a)]^2 cos^2(\theta_1 - \varphi)$. Assuming $t_1 >> \frac{1}{k_{-1} + k_b}$, the excited state $[A^*]$

becomes depleted, and $[A]$ satisfies $[A] = A_0 - [B]$, where $[B] \approx A_0(1 - exp\left(-\frac{k_a k_b}{k_{-1} + k_b} t_1\right)$ computed from $\frac{d[B]}{dt} = k_b[A^*]$, we obtain:

$$[A] \approx A_0 exp\left(-\frac{k_a k_b}{k_{-1} + k_b} t_1\right) = A_0 exp\left(-\frac{I_{expo} \cdot [d_a(h\nu_a)]^2 cos^2(\theta_1 - \varphi) k_b}{k_{-1} + k_b} t_1\right) \equiv \frac{\delta[A]}{\delta\varphi}(\varphi, \theta_1, t_1)$$

Thus, the linear-polarized exposure produces an angularly modulated population of $[A]$, also denoted as $\frac{\delta[A]}{\delta\varphi}(\varphi, \theta_1, t_1)$: it is strongly depleted for $\varphi = \theta_1$ and remains higher for $\varphi = \theta_1 + \pi/2$. The contrast is $1 - exp\left(-\frac{[d_a(h\nu_a)]^2 I_{expo} k_b}{k_{-1} + k_b} t_1\right)$, which represents the part not modulated but bleachable.

Then for subsequent probing with varying polarization θ, the absorption rate is $k_a(h\nu_a, I_{prob}, \theta, \psi) = I_{prob}[d_a(h\nu_a)]^2 cos^2(\theta - \varphi)$.

Therefore,

$$I_{lum}(h\nu_a, h\nu_e, \theta, \theta_1, t1, t) \propto I_{prob} \int_0^{2\pi} [d_a(h\nu_a)]^2 cos^2(\theta - \varphi) exp\left(-\frac{I_{prob}[d_a(h\nu_a)]^2 cos^2(\theta - \varphi) k_b}{k_{-1} + k_b} t\right) exp\left(-\frac{I_{expo}[d_a(h\nu$$

Or with our notations:

$$I_{lum}(h\nu_a, h\nu_e, \theta, \theta_1, t1, t) \propto I_{prob} \int_0^{2\pi} R(h\nu_a, \theta, \varphi) \cdot f(t, I_{prob}, R(h\nu_a, \theta, \varphi)) \cdot f(t_1, I_{expo}, R(h\nu_a, \theta_1, \varphi)) \cdot \frac{\delta A_0}{\delta\varphi} d\varphi$$

To avoid too much bleaching during the probing process, we minimize I_{prob} and t.

This selective bleaching of the distribution clearly induces an anisotropic response in the final luminescence, as illustrated in Fig.S7.

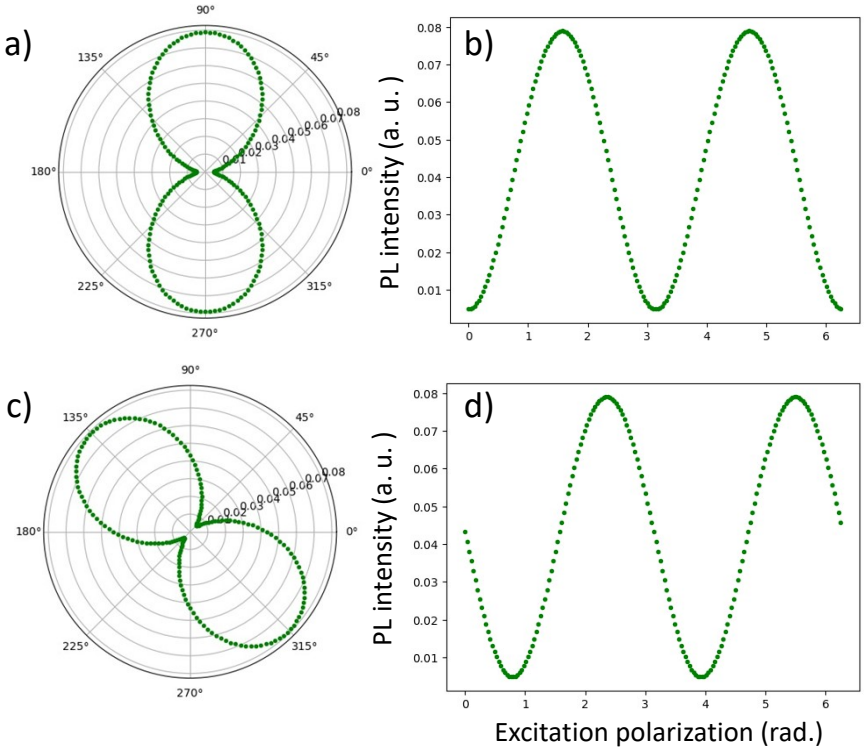

Fig. S7: PL intensity respecting to the probing angle θ during t=1s. The pre-exposure process at θ_1=0° (a)-(b) and 45°(c)-(d) during t_1=100s. Other parameters: I_{prob}=I_{expo}=1, k_0=1, k_{-1}=0.9, k_b=0.1, $\frac{\delta A_0}{\delta \psi} = 1$

Furthermore, if the sample is exposed for a successive period of exposure, supplementary terms $\frac{\delta A_i}{\delta \psi} = f(t_i, I_{prob}, R(h\nu_a, \theta_i, \varphi)) \cdot \frac{\delta A_{i-1}}{\delta \varphi}$ will be added, I_{lum} yields:

$$I_{lum}(h\nu_a, h\nu_e, \theta, \theta_1, t1, t) \propto I_{prob} \int_0^{2\pi} R(h\nu_a, \theta, \varphi) f(t, I_{prob}, R(h\nu_a, \theta, \varphi)) \prod_1^n f(t_i, I_{expo}, R(h\nu_a, \theta_i, \varphi)) \cdot \frac{\delta A_{i-1}}{\delta \varphi} d\varphi$$

Using above equation, results of Fig.3d can be well simulated, as shown in Fig.S8b.

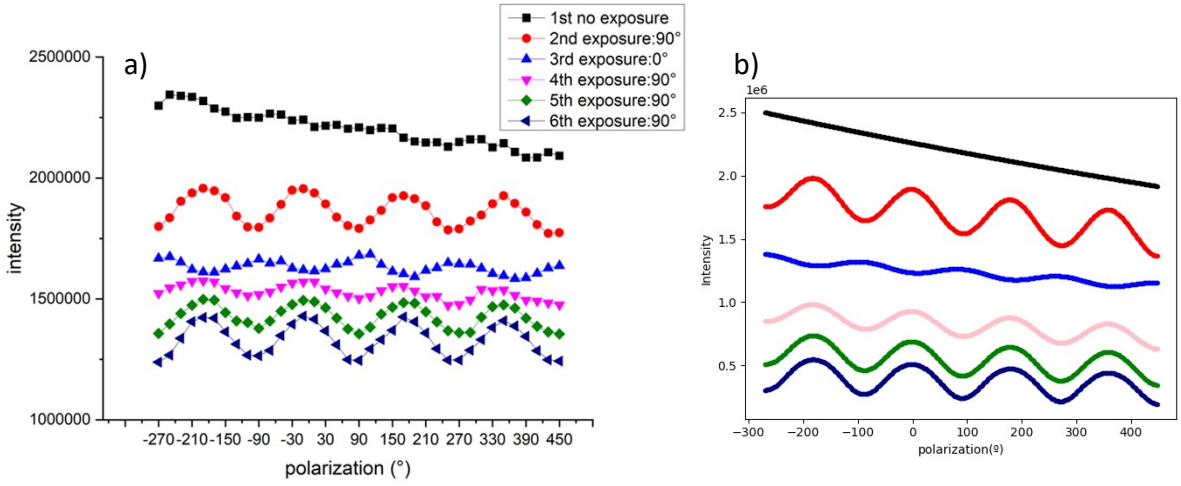

Fig.S8: a) Recall of Fig.3d, the PL intensity probed according to polarization. b) Simulation of Fig. S8(a) using above equation. The parameters are the following: I_{prob}=I_{expo}=0.01, k_0=1, k_{-1}=0.9, k_b=0.1, $A_0 = 10^9$. Probing

time is $t = 180s$, θ_i: $\theta_1 = 90°, \theta_2 = 0°, \theta_3 = \theta_4 = \theta_5 = 90°$, *as the same as the experiment. The exposure time of each step is* $t_1 = 300s, t_2 = 400s, t_3 = 500s, t_4 = 600s, t_5 = 700s$

REFERENCES

[1] J.M. Ha, S.H. Hur, A. Pathak, J.-E. Jeong, H.Y. Woo, Recent advances in organic luminescent materials with narrowband emission, NPG Asia Materials 13 (2021) 53.

[2] R. Que, L. Houel-Renault, M. Temagoult, C. Herrero, M. Lancry, B. Poumellec, Space-selective creation of photonics functions in a new organic material: Femtosecond laser direct writing in Zeonex glass of refractive index change and photoluminescence, Optical Materials 133 (2022) 112651.

[3] B.M.B.B.M.V.V.G. Krasovitskii, Organic luminescent materials, VCH, Weinheim, 1988.

[4] S.J. Strickler, R.A. Berg, Relationship between Absorption Intensity and Fluorescence Lifetime of Molecules, The Journal of Chemical Physics 37 (1962) 814-822.

[5] F.A. Cotton, Chemical applications of group theory, John Wiley & Sons1991.

[6] L.M. Falicov, Group theory and its physical applications, University of Chicago press1966.

[7] M.M. Woolfson, How to use groups by J. W. Leech and D. J. Newman, Acta Crystallographica Section A 25 (1969) 641-641.

[8] F. Weigert, Über einen neuen Effekt der Strahlung, Zeitschrift für Physik 5 (1921) 410-427.